A Method of Retrieving 10-m Spectral Surface Albedo Products from Sentinel-2 and MODIS data

Rui Song
Imaging Group, MSSL
University College London
Surrey, UK
rui.song@ucl.ac.uk

Jan-Peter Muller
Imaging Group, MSSL
University College London
Surrey, UK
j.muller@ucl.ac.uk

Alistair Francis
Imaging Group, MSSL
University College London
Surrey, UK
a.francis.16@ucl.ac.uk

***Abstract*—This study proposed a new method of retrieving 10-m spectral surface albedo products. Three crucial components are incorporated into this high-resolution surface albedo generation system. Firstly, a deep learning system, CloudFCN based on the U-net paradigm has been developed. This produces the best available cloud detection of any algorithm published to date. Secondly, an advanced atmospheric correction model, the Sensor Invariant Atmospheric Correction (SIAC) is employed. The SIAC method considers the surface BRDF effects as these are usually ignored, because the atmosphere correction is a large signal and the largest uncertainty in converting top-of-atmosphere reflectance to top-of-canopy surface reflectance. Thirdly, an endmember-based new technology will be used to retrieve high-resolution albedo from high-resolution reflectance by combining downscaled MODIS BRDF. These methods are further described alongside results shown of the different stages and the final high resolution albedo.**

Keywords: Albedo, Sentinel-2, machine learning, MODIS, SIAC, endmember

I. Introduction

Surface albedo is a fundamental radiative parameter as it controls the Earth's surface energy budget and directly affects the Earth's climate. A new method is proposed of generating 10-m high-resolution spectral surface albedo from Sentinel-2 L1C top-of-atmosphere (TOA) reflectance and MODIS bi-directional reflectance distribution function (BRDF) data. The Sensor Invariant Atmospheric Correction (SIAC) [1] algorithm is developed by, and has been demonstrated (ibid) to greatly improve the accuracy of Sentinel-2 atmospheric correction when compared against the use of in situ AERONET data. The machine learning cloud detection approach CloudFCN [2] is based on a Fully Convolutional Network architecture, and has become a common Deep Learning approach to image segmentation. The CloudFCN exhibits state-of-the- art performance in picking up cloud pixels which is comparable to other methods in terms of performance, speed, and robustness to many different terrain and sensor types. The endmember extraction uses N-FINDR along with the Automatic Target Generation Process to identify pure pixels from Sentinel-2 spectral data. The extracted pure pixels are used to relate the albedo-to-reflectance matrix with the abundance values of different pure pixels. The high-resolution albedo values are finally retrieved by solving this over-parameterised matrix. Within this framework, a MODIS BRDF prior based on 20-years of MCD43A1 and VNP43A1 daily BRDF data is produced (Muller et al., in preparation). This BRDF prior is produced on a daily basis, and will be used to help to provide a temporal interpolation of the high-resolution albedo values over pixels that are covered by clouds. The final processed high-resolution albedo data will be validated over different tower sites where long-time series of in situ albedo products are available.

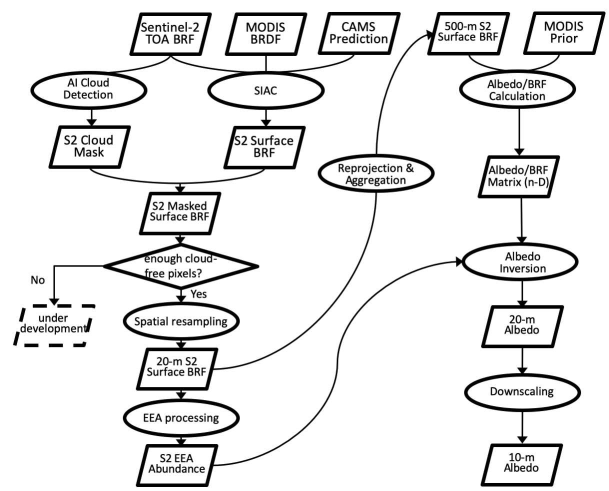

Fig. 1: Processing chain of generating 10m/20m high-resolution albedo products.

II. Method

The high-resolution albedo generation framework consists of five main steps: 1) retrieval of Sentinel-2 spectral surface reflectance using the Sensor Invariant Atmospheric Correction (SIAC) algorithm; 2) generation of Sentinel-2 cloud mask using machine learning; 3) extraction of pure pixels and their corresponding abundance values from 20-m Sentinel-2 data using an Endmember Extraction Algorithm; 4) inversion of high- resolution albedo from MODIS Albedo to Sentinel2 BRF ratio matrix; and 5) downscaling retrieved 20-m spectral and broadband albedo to 10-m. The overall processing chain is described in Fig. 1.

A. SIAC correction

The SIAC atmospheric correction method was developed by Yin et al. [1] from the the Department of Geography at University College London. The main differences between SIAC and traditional atmospheric correction approaches are to be found in the use of an expectation value of surface reflectance at coarse resolution (MODIS MCD43 BRDF kernels), the use of the Copernicus Atmosphere Monitoring Service (CAMS) data as a prior constraint and the use of spatial regularisation in atmospheric composition parameters, along with the use of state-of-the-art atmospheric radiative transfer models through Gaussian Process emulators. SIAC can produce more accurate atmospherically corrected surface reflectance values with estimated uncertainties for each single pixel.

The performance in retrieving Sentinel-2 spectral surface reflectance is compared between the three models: SIAC, Sen2Cor and 6Sv, as shown in Fig. 2. 6Sv uses near-real-time Aerosol Optical Depth (AOD) measurements derived from AERONET in atmospheric corrections. Therefore, 6Sv retrieved spectral surface reflectance values are used as reference measurements in this comparison. The statistical results show that the SIAC corrections have much closer agreement with reference values than the Sent2Cor corrections.

B. Endmember extraction

An endmember is defined as a surface "type" that is assumed to have a unique spectral signature. N-FINDR [4], which is one of earliest endmember extraction algorithms, is employed in this framework to extract pure endmember pixels from Sentinel-2 spectral surface reflectances. Based on the pure spectra that are extracted from N-FINDR, a Fully Constrained Least Squares (FCLS) is employed to estimate the abundance map for each single pure spectrum.

In this framework, Sentinel-2 10m/20m spectral surface reflectance data in band 2 (492.4 nm), 3 (559.8 nm), 4 (664.6 nm), 8A (864.7 nm), 11 (1613.7 nm) and 12 (2202.4 nm) are used as input data for the endmember extraction. Detailed steps for employing endmember extractions on Sentinel-2 data are shown in Fig. 3. This flowchart also shows that the Automatic Target Generation Process (ATGP) [5] is used in initialising the endmembers.

III. Results

Fig. 4 shows an example of a SIAC derived Sentinel-2 surface reflectance in a 10×10 km region centred over the FLUXNET site in Hainich, Germany. The corresponding endmember spectra for this area are shown in Fig. 5. Endmember type-A is classified as vegetation, type-B and type-C are classified as soil, and type-D is classified as bright features (e.g. buildings) in this scene.

The abundance maps for different endmembers are estimated from the FCLS and shown in Fig. 6. As shown in the type-A abundance map, pixels from the Hainich forest have reached an abundance value over 0.9. To evaluate the performance of endmember extractions and abundance estimations,

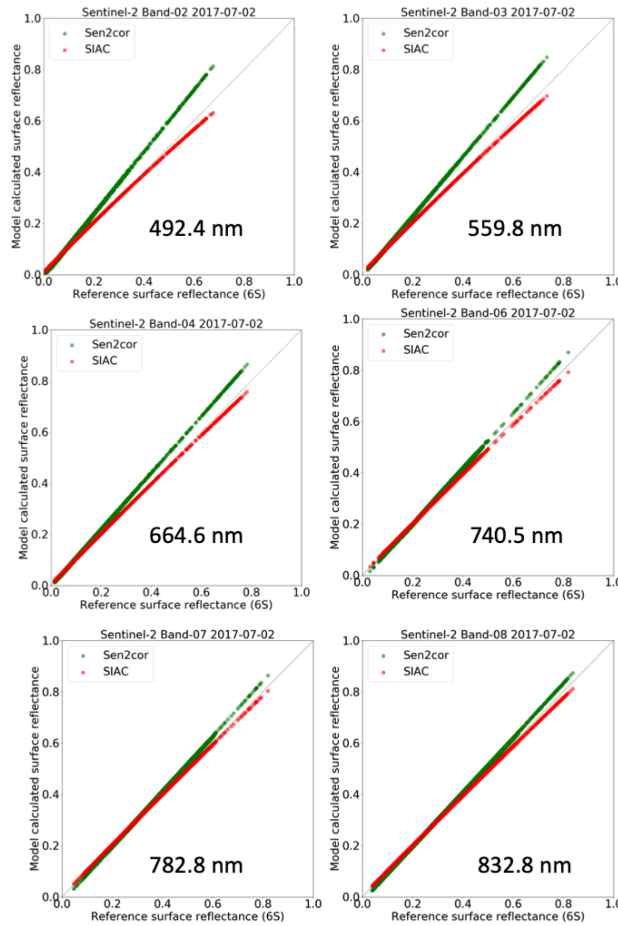

Fig. 2: Comparison of Sentinel-2 spectral surface reflectance values that are retrieved from SIAC (red dots) and Sen2Cor (green dots) [3].

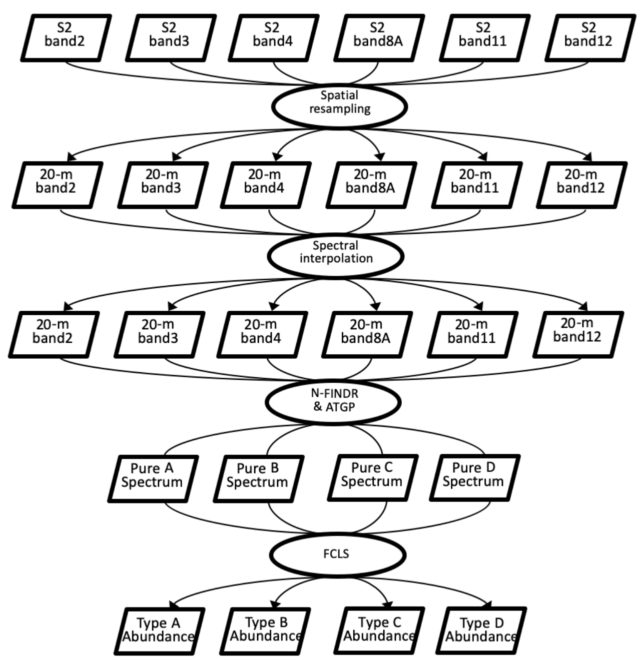

Fig. 3: Flowchart of employing endmember extractions on Sentinel-2 surface reflectance data.

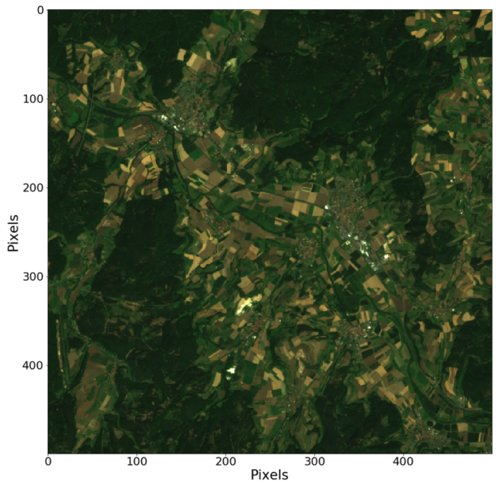

Fig. 4: Example of Sentinel-2 surface reflectance (RGB composition) derived from SIAC corrections in a 10×10 km region.

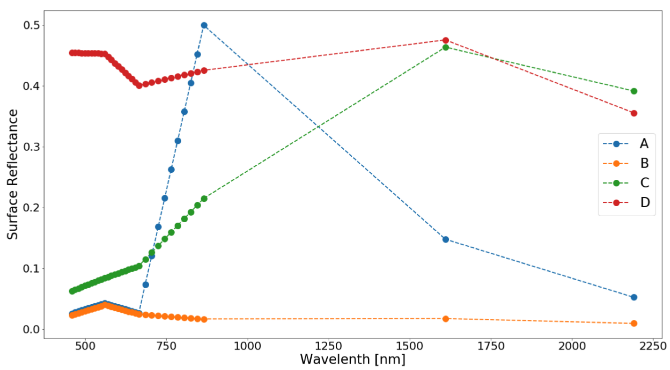

Fig. 5: N-FINDR derived endmember spectra for 4 difference surface types.

the band-to-band BRFs are calculated for different endmember pixels in Fig. 7. It is clearly seen that, the pixel-level band-to-band BRFs are distributed in three different clusters, which means the N-FINDR derived endmembers are pure surface types.

The high-resolution albedo values are retrieved using the method described in [6], [7]. This method uses coarse-resolution albedo values calculated from MODIS BRDF and coarse-resolution surface reflectance values aggregated from Sentinel-2 data, to build a ratio called albedo-to-nadir-reflectance. This ratio is then again used upon high-resolution satellite data to derive the high-resolution surface albedo. In our study, this albedo-to-nadir-reflectance retrieval method is improved by incorporating the use of endmember derived abundance estimations.

Fig. 8 gives an example of the Sentinel-2 high-resolution albedo (DHR and BHR) calculated around the Hainich tower observation site on 6th August, 2015.

IV. Conclusions

This paper introduced a framework for retrieving 10-m spectral surface albedo products from Sentinel-2 and MODIS data.

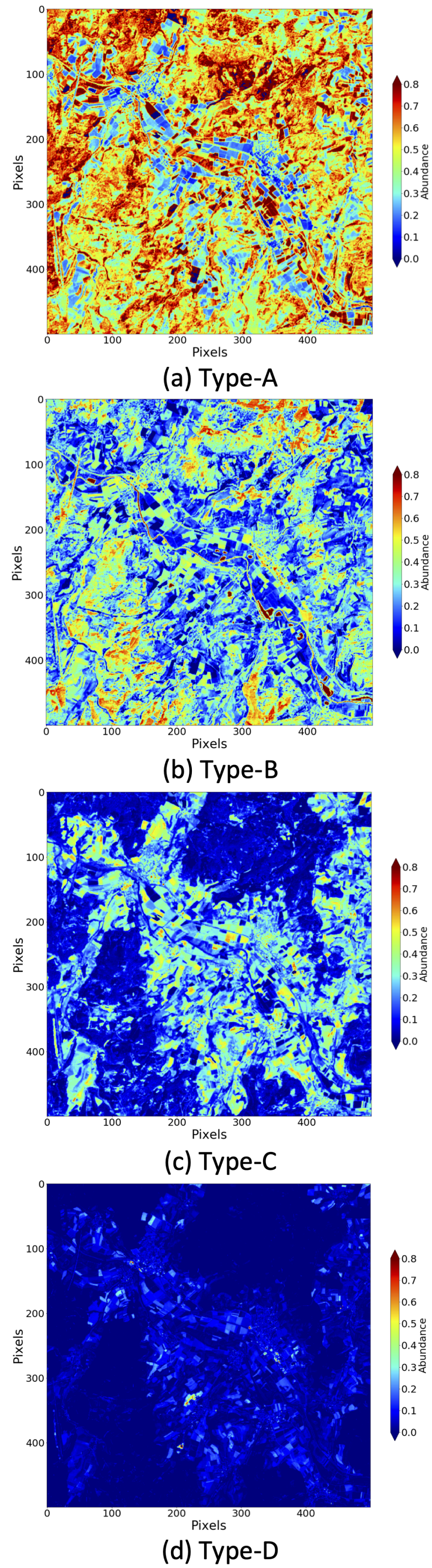

Fig. 6: Endmember abundance map estimated from FCLS.

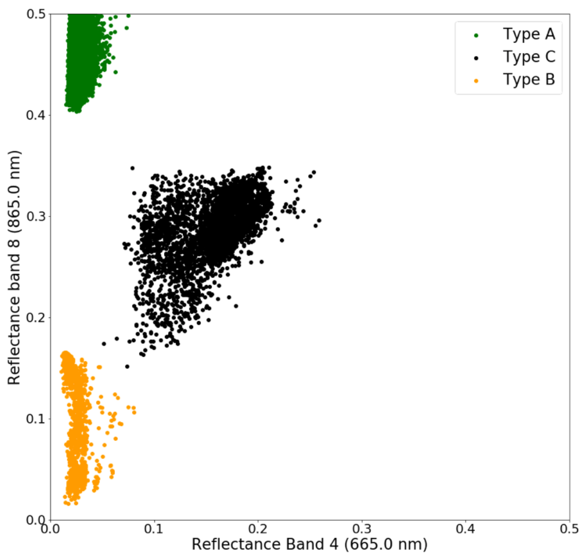

Fig. 7: Band-to-band BRFs for endmember type-A (green dots), type-B (orange dots) and type-C (black dots).

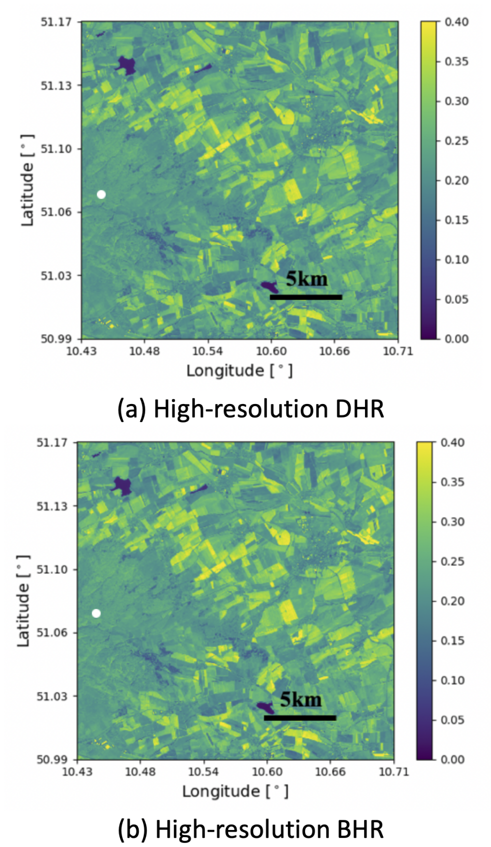

Fig. 8: Calculated high-resolution DHR (a) and BHR (b) over the Hainich site on 6th August, 2015. The white dots indicate the location of the tower.

Based on Sentinel-2 MSI measurements, our putative albedo generation system can produce high temporal and spatial surface albedo products, which offer a great potential for mapping land surface energy budgets especially over agricultural areas. In addition, this high-resolution albedo product can improve the performance of global climate models by providing better constraints on surface albedo parameterisation.

V. Acknowledgements

This work was partly funded by the European Commission Joint Research Centre contract FWC932059, part of the Global Component of the European Union's Copernicus Land Monitoring Service. This work has been undertaken using data processed by the team at UCL for the GBOV project "Ground Based Observation for Validation"(https://land.copernicus.eu/global/gbov). Funding for DE-Hai was provided by the German Federal Ministry of Education and Research (BMBF) as part of the European Integrated Carbon Observation System (ICOS) and by the Deutsche Forschungsgemeinschaft (DFG, INST 186/1118-1 FUGG). We thank the administration of the Hainich National Park for the opportunity for research within the National Park. SIAC was developed with support from European Union Horizon 2020 research and innovation programme under grant agreement No 687320 MULTIPLY (MULTIscale SENTINEL land surface information retrieval Platform). This work was mainly funded by ESA Contract No. 4000130413/20/I-DT (Science in Society project entitled "Generation of high-resolution spectral and broadband surface albedo products based on Sentinel-2 MSI measurements (HR-AlbedoMap)"

References

[1] F. Yin, P. Lewis, J. Gomez-Dans, and Q. Wu, "A sensor-invariant atmospheric correction method: Application to Sentinel-2/MSI and Landsat 8/OLI," *EarthArXiv*, Feb. 2019.

[2] A. Francis, P. Sidiropoulos, and J.-P. Muller, "Cloudfcn: Accurate and robust cloud detection for satellite imagery with deep learning," *Remote Sensing*, vol. 11, no. 19, 2019.

[3] R. Song, J.-P. Muller, S. Kharbouche, F. Yin, W. Woodgate, M. Kitchen, M. Roland, N. Arriga, W. Meyer, G. Koerber, D. Bonal, B. Burban, A. Knohl, L. Siebicke, P. Buysse, B. Loubet, M. Leonardo, C. Lerebourg, and N. Gobron, "Validation of space-based albedo products from upscaled tower-based measurements over heterogeneous and homogeneous landscapes," *Remote Sensing*, vol. 12, no. 5, 2020.

[4] M. E. Winter, "N-FINDR: an algorithm for fast autonomous spectral endmember determination in hyperspectral data," in *Imaging Spectrometry V*, M. R. Descour and S. S. Shen, Eds., vol. 3753, International Society for Optics and Photonics. SPIE, 1999, pp. 266 – 275. [Online]. Available: https://doi.org/10.1117/12.366289

[5] A. Plaza and C. . Chang, "Impact of initialization on design of endmember extraction algorithms," *IEEE Transactions on Geoscience and Remote Sensing*, vol. 44, no. 11, pp. 3397–3407, 2006.

[6] Y. Shuai, J. G. Masek, F. Gao, C. B. Schaaf, and T. He, "An approach for the long-term 30-m land surface snow-free albedo retrieval from historic landsat surface reflectance and modis-based a priori anisotropy knowledge," *Remote Sensing of Environment*, vol. 152, pp. 467 – 479, 2014.

[7] Z. Li, A. Erb, Q. Sun, Y. Liu, Y. Shuai, Z. Wang, P. Boucher, and C. Schaaf, "Preliminary assessment of 20-m surface albedo retrievals from sentinel-2a surface reflectance and modis/viirs surface anisotropy measures," *Remote Sensing of Environment*, vol. 217, pp. 352 – 365, 2018.